

## ON A REGULARIZATION SCHEME FOR LINEAR OPERATORS IN DISTRIBUTION SPACES WITH AN APPLICATION TO THE SPHERICAL RADON TRANSFORM\*

THOMAS SCHUSTER<sup>†</sup> AND ERIC TODD QUINTO<sup>‡</sup>

**Abstract.** This article provides a framework to regularize operator equations of the first kind where the underlying operator is linear and continuous between distribution spaces, the dual spaces of smooth functions. To regularize such a problem, the authors extend Louis' method of approximate inverse from Hilbert spaces to distribution spaces. The idea is to approximate the exact solution in the weak topology by a smooth function, where the smooth function is generated by a mollifier. The resulting regularization scheme consists of the evaluation of the given data at so-called reconstruction kernels which solve the dual operator equation with the mollifier as right-hand side. A nontrivial example of such an operator is given by the spherical Radon transform which maps a function to its mean values over spheres centered on a line or plane. This transform is one of the mathematical models in sonar and radar. After establishing the theory of the approximate inverse for distributions, we apply it to the spherical Radon transform. The article also contains numerical results.

**Key words.** spherical Radon transform, sonar, distribution, regularization, approximate inverse, mollifier, reconstruction kernel

**AMS subject classifications.** 44A12, 45A05, 46F12

**DOI.** 10.1137/S003613990343879X

**1. Introduction.** We apply the method of approximate inverse to the problem of reconstructing a function from integrals over spheres. Applications of this mathematical problem include sonar when the source and detector are at the same point [15], thermoacoustic tomography for cancer detection [14], seismic testing [23], and radar. The article [5] provides an excellent introduction to synthetic aperture radar and the relation between spherical integrals and radar and sonar.

The approximate inverse was originally developed by Louis as a general method to regularize ill-posed operators on Hilbert spaces [17]. It has been applied to integral equations of the first kind [18] and tomography [27, 28]. However, the inversion formula for our problem is valid not on Hilbert spaces but on distributions. Therefore, we will generalize the approximate inverse to the setting of distributions. It is hoped this generalization will be useful for other inverse problems for which the ambient spaces are not Hilbert spaces.

In seismology or sonar the acoustic wave equation is

$$n^2(x)u_{tt} = \Delta u + \delta(t)\delta(x - a_0), \text{ where } a_0 \in A,$$

and  $A$  is a small section of the surface of the earth. After linearization, the determination of  $n^2(x)$  from back-scattered data is equivalent to recovering  $n^2$  from integrals

---

\*Received by the editors December 15, 2003; accepted for publication (in revised form) September 14, 2004; published electronically April 26, 2005. This material is based on work supported by the National Science Foundation under NSF grant DMS 0200788 and support from Tufts University FRAC.

<http://www.siam.org/journals/siap/65-4/43879.html>

<sup>†</sup>Tufts University, Department of Mathematics. Permanent address: Institut für Angewandte Mathematik, Universität des Saaleandes, 66041, Saarbrücken, Germany (thomas.schuster@num.uni-sb.de). The research of this author was partially supported by a Feodor Lynen Fellowship of the Alexander von Humboldt Foundation under V-3.FLF-DEU/1073550.

<sup>‡</sup>Tufts University, Department of Mathematics, 503 Boston Avenue, Medford, MA 02155 (todd.quinto@tufts.edu).

over spheres with centers on  $A$  [15]. Knowing  $n^2$  or at least an approximation to  $n^2$  can show boundaries of objects in the water. This linearized model is reasonable from a practical standpoint when the speed of sound in the ambient water is fairly constant. This would occur in water of depth less than 100 feet with fairly constant temperature [3]. Since the speed of sound is constant in shallow water with constant temperature, a pulse travels from a point source,  $a$ , making a spherical wavefront. The sound that is reflected back to the source at time  $t$  gives the amount reflected back from the sphere centered at  $a$  and radius  $t/2$  times the speed of sound (assuming no multiple reflections). See [12] for practical information about sonar.

The mathematical problem can be described as trying to recover a function by its integrals over all spheres centered on a given line (in  $\mathbb{R}^2$ ), plane (in  $\mathbb{R}^3$ ), or hyperplane (in  $\mathbb{R}^n$ ).

We first discuss the inversion methods that have been implemented numerically and then the pure mathematical results behind them. Denisjuk has an inversion method based on a transformation that changes the spherical transform into a limited data line transform [9]. He has implemented his method with good results. Klein [13] has developed and numerically tested a promising inversion method based on the ideas of Andersson discussed below. Beltukov proposed a numerical inversion method using a discrete SVD for the sonar transform [4]. He showed that the singular values are fairly flat and then drop off precipitously, which reflects the ill-posedness of the problem.

Our numerical reconstructions are given in section 6 and they show the potential of our method.

Many authors have proven injectivity and inversion methods for this transform. Courant and Hilbert [7, p. 699] proved injectivity for functions that are even about the hyperplane. Fawcett [10] and Andersson [2] provide inversion formulas in  $\mathbb{R}^n$ . Norton provides an inversion method for the circular transform if the center set is a circle in the plane [22] and if the center set is a line [21], and [23] gives three-dimensional results. Ranges and inversion formulas on a subspace of Schwartz functions are given in [20].

Finch, Patch, and Rakesh [11] develop an explicit inversion formula for recovering a function from spherical integrals when the center set is the boundary of a bounded, connected, open set in  $\mathbb{R}^n$ . Ramm proves injectivity and inversion theorems in [26]. Fairly general uniqueness theorems are given in [1].

Louis and Quinto [19] develop the microlocal analysis of the transform when  $A$  is a real-analytic surface (e.g., an open subset of a hyperplane), and they prove the local transform is injective under fairly general hypotheses. They characterize singularities (jumps, etc.) of the object that are stably visible from the data. Palamodov [24] and Denisjuk [8] continue this microlocal analysis when  $S$  is a hyperplane, providing instability results, inversion methods, and range theorems. Beltukov has proven an inversion method for the transform on hyperbolic space.

Section 2 contains the extension of the method of approximate inverse to distribution spaces. In particular, we define what we mean by a mollifier in the distributional sense. In section 3, we apply this concept to the inverse problem of inverting the spherical Radon transform. Section 4 deals with the design of a mollifier for this problem. The computation of the corresponding reconstruction kernel is outlined in section 5. Section 6 provides a couple of numerical tests using synthetic Radon data, and the proof that our functions satisfy the conditions to be mollifiers is in the appendix.

**2. Approximate inverse in distribution spaces.** In this section we extend the method of approximate inverse as introduced by Louis and Maass [18] and Louis [16, 17] to distribution spaces.

To this end let  $\Omega_1 \subset \mathbb{K}^n$ ,  $\Omega_2 \subset \mathbb{K}^m$  be open sets,  $\mathbb{K} = \mathbb{R}$  or  $\mathbb{K} = \mathbb{C}$ , and  $V \subset \mathcal{C}^\infty(\Omega_1)$ ,  $W \subset \mathcal{C}^\infty(\Omega_2)$  be subspaces which are closed in their own topology. We denote the dual spaces (continuous linear functionals) for  $V$  and  $W$  by  $V'$ ,  $W'$ , respectively. Furthermore we assume  $A : V' \rightarrow W'$  to be a linear mapping which is one-to-one. The inverse problem under consideration is as follows. Given a  $g \in W'$  lying in the range  $A(V')$  of  $A$ , find  $f \in V'$  such that

$$(2.1) \quad Af = g.$$

The concept of approximate inverse involves so called *mollifiers*. The aim is to calculate convolutions of them with the sought solution  $f$  rather than to calculate  $f$  itself. To extend this concept to distribution spaces  $V', W'$  we first define what we mean by a mollifier.

DEFINITION 2.1. For  $\gamma > 0$  let  $e_\gamma(\cdot, y) \in V''$  for all  $y \in \Omega_1$  such that

$$(2.2) \quad \langle \varphi, e_\gamma(\cdot, y) \rangle_{V' \times V''} \in V' \quad \text{for all } \varphi \in V'.$$

We call  $e_\gamma$  a mollifier if and only if

$$(2.3) \quad \langle \langle \varphi, e_\gamma(\cdot, y) \rangle_{V' \times V''}, \beta \rangle_{V' \times V} \rightarrow \langle \varphi, \beta \rangle_{V' \times V}$$

as  $\gamma \rightarrow 0$  for all  $\beta \in V$ .

Let  $V_1 \subset V'$  and let  $V_2 \subset V$ . Then,  $e_\gamma$  is a  $(V_1, V_2)$ -mollifier if and only if (2.2) holds for all  $\varphi \in V_1$  and (2.3) holds for all  $\varphi \in V_1$  and  $\beta \in V_2$ .

In Definition 2.1 we denote the double dual of  $V$  by  $V''$ , and  $\langle \cdot, \cdot \rangle_{V' \times V}$ ,  $\langle \cdot, \cdot \rangle_{V' \times V''}$  are the corresponding dual pairings.

If  $e_\gamma$  is a mollifier in the sense of Definition 2.3, then for  $f \in V'$ ,

$$(2.4) \quad f_\gamma(y) := \langle f, e_\gamma(\cdot, y) \rangle_{V' \times V''}, \quad y \in \Omega_1,$$

is a distribution in  $V'$  which converges to  $f$  in the (weak) topology of  $V'$ . Because  $V \subset V''$ ,  $e_\gamma$  can be chosen from  $V$ . Thus,  $f_\gamma$  is a kind of smooth version of  $f$ . If  $e_\gamma$  is a  $(V_1, V_2)$ -mollifier, then (2.4) holds for all  $f \in V_1$  and convergence holds when tested against all  $\beta \in V_2$ .

To obtain  $f_\gamma$  from  $Af$  we consider the adjoint operator of  $A$ . Since  $A : V' \rightarrow W'$  is linear, continuous, and one-to-one, it has a linear and continuous adjoint  $A^* : W'' \rightarrow V''$  with dense range. Suppose that for each  $y \in \Omega_1$  we have an element  $\Psi_\gamma(y) \in W''$  satisfying

$$(2.5) \quad A^*\Psi_\gamma(y) = e_\gamma(\cdot, y).$$

Then,  $f_\gamma$  can be expressed as

$$\begin{aligned} f_\gamma(y) &= \langle f, e_\gamma(\cdot, y) \rangle_{V' \times V''} = \langle f, A^*\Psi_\gamma(y) \rangle_{V' \times V''} \\ &= \langle Af, \Psi_\gamma(y) \rangle_{W' \times W''} = \langle g, \Psi_\gamma(y) \rangle_{W' \times W''}, \end{aligned}$$

where  $g = Af$  are the given data. The mapping  $S_\gamma : W' \rightarrow V'$  defined by

$$(2.6) \quad S_\gamma g = \langle g, \Psi_\gamma(y) \rangle_{W' \times W''}$$

is called the *approximate inverse* of  $A$ ; the element  $\Psi_\gamma(y)$  is the *reconstruction kernel* corresponding to  $e_\gamma$ . Thus, the approximate inverse consists of evaluations of dual pairings of the given data  $g$  and the reconstruction kernels  $\Psi_\gamma(y)$ .

Three main features of the approximate inverse are as follows:

- The reconstruction kernels  $\Psi_\gamma(y)$  can be precomputed before the measurement process starts.
- Equation (2.5) is independent of the data  $g$  and hence not influenced by noise.
- Invariance properties of  $A^*$  help to improve the efficiency of the method, if (2.5) has to be solved only for one single  $y \in \Omega_1$ . We will demonstrate this in section 3.

REMARK 2.2. *In general, it does not follow that choosing a mollifier  $e_\gamma$  from  $V$  results in a reconstruction kernel  $\Psi_\gamma(y) \in W$ . The key is that (2.5) must have a solution in  $W$ . If  $A^*(W) \cap V$  is dense in  $V$ , then this is more likely. This density condition will happen if the adjoint  $A^*$  maps  $W$  to  $V \subset V''$ .*

In practical situations we have only finitely many measurement data available rather than a distribution  $g$ . For this reason investigating the semidiscrete operator equation

$$(2.7) \quad A_N f = g_N,$$

where  $A_N = \Phi_N A$ ,  $g_N = \Phi_N g \in \mathbb{K}^N$ , may fit better to that situation. Here, the observation operator  $\Phi_N \in W''$  can be, e.g., point evaluations, if  $A(V')$  consists of continuous, not necessarily integrable, functions. But following the outlines of Rieder and Schuster [27, 28] we formulate the approximate inverse of (2.7) by

$$(2.8) \quad S_{\gamma,N} g_N(y) = \langle g_N, G_N \Phi_N \Psi_\gamma(y) \rangle_{\mathbb{K}^N},$$

where  $\Psi_\gamma(y)$  is a reconstruction kernel for (2.1) and  $G_N \in \mathbb{K}^{N \times N}$  is a matrix containing the weights of a numerical integration rule which is applied to get the discrete version (2.8) of the dual pairing  $\langle \cdot, \cdot \rangle_{W' \times W''}$ . Thus, we continue in this article to focus on the continuous problem.

REMARK 2.3. *Compared to the concept of approximate inverse in Hilbert spaces as established by Louis [16], Definition 2.1 applies to more general spaces and requires less restrictive assumptions on an element  $e_\gamma$  to be a mollifier. The  $L^2$ -theory requires convergence of  $f_\gamma(y) = \langle f, e_\gamma(\cdot, y) \rangle \rightarrow f(y)$  in  $L^2$  as  $\gamma \rightarrow 0$ , but this distributional setup requires only weak convergence. We should point out that our theory is meant for distribution spaces and does not directly subsume the  $L^2$ - or  $H^s$ -theory since these Hilbert spaces are not closed subspaces of distribution spaces, the topologies are too different, and their standard duals are not their duals as distribution spaces. It should also be pointed out that this generalization to distributions is necessary for the spherical transform since the transform does not map  $L^2$  into  $L^2$  and the inversion formula we use applies to distributions.*

**3. Approximate inverse meets the spherical Radon transform.** In this section we apply the method of approximate inverse established in section 2 to the spherical Radon transform. We use the mathematical setup of Andersson's article [2] and formulate some of his main results first.

We start with some notation. Throughout the paper a scalar product  $\langle \cdot, \cdot \rangle$  or norm  $\| \cdot \|$  without subscript always means the Euclidean scalar product or norm, respectively. We denote the space of all rapidly decreasing, smooth functions by  $\mathcal{S}(\mathbb{R}^n)$  and give this space the usual seminorms [29, section 7.3]. This topology turns  $\mathcal{S}(\mathbb{R}^n)$  into a Fréchet space. The Fourier transform  $F : \mathcal{S}(\mathbb{R}^n) \rightarrow \mathcal{S}(\mathbb{R}^n)$  and its inverse are given by

$$Ff(\xi) = \hat{f}(\xi) = \int_{\mathbb{R}^n} f(x) e^{-i \langle \xi, x \rangle} dx, \quad F^{-1}f(x) = (2\pi)^{-n} \int_{\mathbb{R}^n} f(\xi) e^{i \langle x, \xi \rangle} d\xi.$$

The dual space  $\mathcal{S}'(\mathbb{R}^n)$  of  $\mathcal{S}(\mathbb{R}^n)$  is called the set of *tempered distributions*. Each distribution  $\varphi \in \mathcal{S}'(\mathbb{R}^n)$  is of finite order [29] and can be written as the derivative of a continuous function of polynomial growth [6].

The Fourier transform gives isomorphisms on  $\mathcal{S}(\mathbb{R}^n)$  and on  $\mathcal{S}'(\mathbb{R}^n)$ . Finally, we often write a vector  $x \in \mathbb{R}^{n+1}$  in the form  $x = (x', x_{n+1})^\top$ , where  $x' = (x_1, \dots, x_n)^\top \in \mathbb{R}^n$  contains the first  $n$  components of  $x$  and  $x_{n+1}$  is the last component. We will drop the  $\top$  when this correspondence is clear.

The *spherical Radon transform*  $R$  assigns a function  $f \in \mathcal{S}(\mathbb{R}^{n+1})$  its mean values over all spheres centered about  $(z, 0) \in \mathbb{R}^{n+1}$ ,  $z \in \mathbb{R}^n$  with radius  $r \geq 0$ :

$$(3.1) \quad Rf(z, r) = \frac{1}{\omega_n} \int_{S^n} f(z + r\xi, r\eta) dS_n(\xi, \eta) = g(z, r).$$

Here,  $\omega_n$  is the area of the  $n$ -dimensional sphere  $S^n = \{(\xi, \eta) \in \mathbb{R}^{n+1} : \xi \in \mathbb{R}^n, \eta \in \mathbb{R}, \|\xi\|^2 + \eta^2 = 1\}$  and  $dS_n$  is the surface measure on  $S^n$ .

Obviously  $Rf = 0$  holds true for every  $f \in \mathcal{S}(\mathbb{R}^{n+1})$  that is odd in the last variable:  $f(x', -x_{n+1}) = -f(x', x_{n+1})$ . Courant and Hilbert [7] proved that the kernel of  $R$  consists exactly of all such functions. This suggests restricting  $R$  to the subspace of even functions in the last variable,

$$\mathcal{S}_e := \mathcal{S}_e(\mathbb{R}^{n+1}) = \{f \in \mathcal{S}(\mathbb{R}^{n+1}) : f(x', -x_{n+1}) = f(x', x_{n+1})\}.$$

Unfortunately, even if  $f \in \mathcal{S}_e(\mathbb{R}^{n+1})$ , the image  $Rf$  does not have to be in  $L^2(\mathbb{R}^{n+1})$ . In fact, if  $f$  is the characteristic function of a circle, then  $Rf$  has infinite support and does not decrease at infinity. Furthermore, one can show (e.g., using ideas in [19, 24]) that  $R^{-1}$  is not continuous in any range of Sobolev norms, at least with data for bounded centers or radii (see Remark 2.3).

Identifying the radius  $r$  in (3.1) with the norm  $\|w\|$  of a vector  $w \in \mathbb{R}^{n+1}$ , we introduce the following subspace of  $\mathcal{S}(\mathbb{R}^{2n+1})$ :

$$\begin{aligned} \mathcal{S}_r &:= \mathcal{S}_r(\mathbb{R}^n \times \mathbb{R}^{n+1}) \\ &= \{f \in \mathcal{S}(\mathbb{R}^{2n+1}) : f(z, w) = \check{f}(z, \|w\|) \text{ for a function } \check{f} \in \mathcal{S}_e(\mathbb{R}^{n+1})\}. \end{aligned}$$

Thus,  $\mathcal{S}_r(\mathbb{R}^n \times \mathbb{R}^{n+1})$  consists of the functions in  $\mathcal{S}(\mathbb{R}^{2n+1})$  which are radially symmetric in the last  $n + 1$  variables. We will often view functions in  $\mathcal{S}_r(\mathbb{R}^n \times \mathbb{R}^{n+1})$  as functions on  $\mathbb{R}^n \times \mathbb{R}$  where we write  $f(z, r) = f(z, w)$  with  $r = \|w\|$ , but when we take the Fourier transform, it will be the Fourier transform on  $\mathbb{R}^{2n+1}$ .

As mentioned before, we cannot expect that  $Rf \in \mathcal{S}_r(\mathbb{R}^n \times \mathbb{R}^{n+1})$  even when  $f \in \mathcal{S}_e(\mathbb{R}^{n+1})$ . But it is easy to show that  $Rf \in \mathcal{S}'_r(\mathbb{R}^n \times \mathbb{R}^{n+1})$ , the dual space of  $\mathcal{S}_r(\mathbb{R}^n \times \mathbb{R}^{n+1})$ . By a density argument we may extend  $R$  to domain  $\mathcal{S}'_e(\mathbb{R}^{n+1})'$ . The following theorem summarizes some properties of  $R$  considered as mapping between  $\mathcal{S}'_e$  and  $\mathcal{S}'_r$ . The proofs are in [2] or [13].

**THEOREM 3.1** (see [2, Theorem 2.1 and Proposition 2.2]). *The spherical Radon transform  $R : \mathcal{S}'_e \rightarrow \mathcal{S}'_r$  is a linear, continuous operator which is one-to-one and has range*

$$(3.2) \quad R(\mathcal{S}'_e) = \mathcal{S}'_{r,cone} := \left\{ g \in \mathcal{S}'_r : \text{supp } \hat{g} \subset \{(\sigma, \rho) \in \mathbb{R}^n \times [0, \infty) : \rho \geq \|\sigma\|\} \right\} \subset \mathcal{S}'_r.$$

*If the Fourier transform of  $f \in \mathcal{S}'_e$  is equal to an integrable function  $\hat{f}(\sigma, \omega)$ , then the inversion formula*

$$(3.3) \quad \hat{f}(\sigma, \omega) = c_n |\omega| (\|\sigma\|^2 + \omega^2)^{(n-1)/2} \hat{g}(\sigma, \sqrt{\|\sigma\|^2 + \omega^2})$$

*is valid with  $c_n = \omega_n / (2(2\pi)^n)$  and  $g = Rf$ .*

The adjoint operator  $R^* : \mathcal{S}_r \rightarrow \mathcal{S}_e$  has dense range and is given by

$$(3.4) \quad R^*g(x', x_{n+1}) = \int_{\mathbb{R}^n} g\left(z, \sqrt{\|z - x'\|^2 + x_{n+1}^2}\right) dz;$$

its Fourier transform is

$$(3.5) \quad FR^*g(\sigma, \rho) = \hat{g}(\sigma, \sqrt{\|\sigma\|^2 + \rho^2}).$$

Note that the right-hand side of (3.3) is the Fourier transform of the function  $g$  in  $\mathbb{R}^{2n+1}$  that is radial in the last  $n + 1$  variables. The reason to consider  $R$  as a map into  $\mathcal{S}'_r(\mathbb{R}^n \times \mathbb{R}^{n+1})$  rather than  $\mathcal{S}'_e(\mathbb{R}^{n+1})$  is that the relationship between the Fourier transform and spherical transform is easier in these spaces. The constant  $c_n$  in (3.3) differs from the corresponding constant in Andersson’s article by a factor of  $(2\pi)^{-n}$ . This inaccuracy was found by Klein [13].

In order to apply the approximate inverse (section 2) to solve the inverse problem of finding a distribution  $f \in \mathcal{S}'_e$  satisfying

$$(3.6) \quad Rf = g$$

for a given  $g \in \mathcal{S}'_r$  in the range of  $R$ , we identify  $V = \mathcal{S}_e$ ,  $W = \mathcal{S}_r$ , and  $A = R$ . Note that due to Theorem 3.1,  $R^*$  maps  $\mathcal{S}_r$  into  $\mathcal{S}_e$  and we have the situation mentioned in Remark 2.2 and may choose a mollifier  $e_\gamma(\cdot, y) \in \mathcal{S}_e$  for every  $y \in \mathbb{R}^{n+1}$ . Once having a mollifier  $e_\gamma$  at hand, the following extension lemma, whose proof also can be found in [2], helps us to find a solution of the equation

$$(3.7) \quad R^*\Psi_\gamma(y) = e_\gamma(\cdot, y),$$

which is our reconstruction kernel; see (2.5).

LEMMA 3.2 (see [2, Extension Lemma 2.4 and Corollary 2.5]). *There exists a continuous linear mapping  $E : \mathcal{S}_e \rightarrow \mathcal{S}_r$  such that*

$$(3.8) \quad R^*E = id_{\mathcal{S}_e}.$$

For  $\rho \geq \|\sigma\|$  the mapping  $E$  satisfies

$$(3.9) \quad FEf(\sigma, \rho) = \hat{f}(\sigma, \sqrt{\rho^2 - \|\sigma\|^2}).$$

If  $e_\gamma(\cdot, y) \in \mathcal{S}_e$  is a mollifier in the sense of Definition 2.1, then the reconstruction kernel  $\Psi_\gamma(y)$  belonging to  $e_\gamma$  is given by

$$(3.10) \quad \Psi_\gamma(y) = Ee_\gamma(\cdot, y).$$

With the help of (3.8) we easily see that  $\Psi_\gamma(y)$  from (3.10) is a solution of (3.7).

From (3.5), it is clear that any continuous  $E$  that satisfies (3.9) will satisfy (3.8). We will choose  $E$  so that for a mollifier  $e_\gamma(\cdot, y)$  in  $\mathcal{S}_e$ ,  $Ee_\gamma(\cdot, y)$  is in  $\mathcal{S}_r$ .

So far we know how to get the reconstruction kernel once we have chosen a mollifier. Theorem 4.1 will provide general criteria that will allow us to construct mollifiers, and with the help of Lemma 3.2 we know how to find a corresponding solution of (3.7). But it would be very time-consuming if we had to solve (3.7) for all reconstruction points  $y$ . To this end we prove an invariance property of  $R^*$ , Lemma 3.3, which allows us to solve (3.7) only once and to generate *all* reconstruction kernels by applying the invariance to that *one* solution.

For a given  $M > 1$ , we denote

$$\begin{aligned} \mathcal{H}^M &= \mathcal{H}^M(\mathbb{R}^{n+1}) = \{y = (y', y_{n+1}) \in \mathbb{R}^{n+1} : 1/M < |y_{n+1}|\}, \\ (3.11) \quad \mathcal{H}^{M,M} &= \mathcal{H}^{M,M}(\mathbb{R}^{n+1}) = \{y = (y', y_{n+1}) \in \mathbb{R}^{n+1} : 1/M < |y_{n+1}| < M\}. \end{aligned}$$

Furthermore, if  $U \subset \mathbb{R}^{n+1}$  is open, we define

$$\begin{aligned} \mathcal{S}_e(U) &= \{f \in \mathcal{S}_e(\mathbb{R}^{n+1}) : \text{supp } f \subset U\}, \\ \mathcal{S}'_e(U) &= \{f \in \mathcal{S}'_e(\mathbb{R}^{n+1}) : \text{supp } f \subset U\}, \\ \mathcal{E}'_e(U) &= \{f \in \mathcal{S}'_e(\mathbb{R}^{n+1}) : \text{supp } f \subset U \text{ is compact}\}. \end{aligned}$$

Note that, in general,  $\mathcal{S}'_e(U)$  is a proper subspace of the dual space of  $\mathcal{S}_e(U)$ .

We define mappings  $\mathcal{S}_e^y : \mathcal{S}_e \rightarrow \mathcal{S}_e$  and  $\mathcal{S}_r^y : \mathcal{S}_r \rightarrow \mathcal{S}_r$  by

$$(3.12) \quad \mathcal{S}_e^y f(x) = \begin{cases} |y_{n+1}|^{-n-1} f\left(\frac{x'-y'}{|y_{n+1}|}, \frac{x_{n+1}}{|y_{n+1}|}\right), & y \in \mathcal{H}^M(\mathbb{R}^{n+1}), \\ 0, & y \notin \mathcal{H}^M(\mathbb{R}^{n+1}), \end{cases}$$

$$(3.13) \quad \mathcal{S}_r^y g(z, r) = \begin{cases} |y_{n+1}|^{-2n-1} g\left(\frac{z-y'}{|y_{n+1}|}, \frac{r}{|y_{n+1}|}\right), & y \in \mathcal{H}^M(\mathbb{R}^{n+1}), \\ 0, & y \notin \mathcal{H}^M(\mathbb{R}^{n+1}). \end{cases}$$

Because  $\mathcal{S}_e^y$  and  $\mathcal{S}_r^y$  are compositions of dilations and translations, they are linear and continuous mappings on  $\mathcal{S}_e$  and  $\mathcal{S}_r$ , respectively. Moreover, both operators intertwine with the adjoint  $\mathcal{R}^*$ . It is also clear that  $\mathcal{S}_e^y f$  and  $\mathcal{S}_r^y g$  can be discontinuous in  $y$  for  $y_{n+1} = \pm 1/M$ .

LEMMA 3.3. *Let  $\mathcal{S}_e^y : \mathcal{S}_e \rightarrow \mathcal{S}_e$  and  $\mathcal{S}_r^y : \mathcal{S}_r \rightarrow \mathcal{S}_r$  be defined as in (3.12) and (3.13), respectively. Then,*

$$(3.14) \quad \mathcal{S}_e^y \mathcal{R}^* = \mathcal{R}^* \mathcal{S}_r^y.$$

*Proof.* Let  $y \in \mathcal{H}^M(\mathbb{R}^{n+1})$ . Using representation (3.4) together with the definitions (3.12) and (3.13) gives

$$\begin{aligned} \mathcal{R}^* \mathcal{S}_r^y g(x', x_{n+1}) &= |y_{n+1}|^{-2n-1} \int_{\mathbb{R}^n} g\left(\frac{z-y'}{|y_{n+1}|}, |y_{n+1}|^{-1} \sqrt{\|z-x'\|^2 + x_{n+1}^2}\right) dz \\ &= |y_{n+1}|^{-n-1} \int_{\mathbb{R}^n} g\left(z, \sqrt{\|z - |y_{n+1}|^{-1}(x' - y')\|^2 + |y_{n+1}|^{-2} x_{n+1}^2}\right) dz \\ &= \mathcal{S}_e^y \mathcal{R}^* g(x', x_{n+1}) \end{aligned}$$

for all  $g \in \mathcal{S}_r$ . For  $y \notin \mathcal{H}^M(\mathbb{R}^{n+1})$  assertion (3.14) follows immediately, since both sides are equal to zero.  $\square$

Lemma 3.3 tells us that under certain conditions we may restrict ourselves to solving (3.7) only for *one single*  $y \in \mathbb{R}^{n+1}$ .

COROLLARY 3.4. *For each  $\gamma > 0$  let  $\bar{e}_\gamma \in \mathcal{S}_e(\mathbb{R}^{n+1})$  and  $e_\gamma(\cdot, y) \in \mathcal{S}_e$  be defined by  $\mathcal{S}_e^y$ :*

$$(3.15) \quad e_\gamma(x, y) = \mathcal{S}_e^y \bar{e}_\gamma(x).$$

*Assume  $e_\gamma$  is a mollifier. Then, we get all corresponding reconstruction kernels by solving*

$$(3.16) \quad \mathcal{R}^* \bar{\Psi}_\gamma = \bar{e}_\gamma$$

and setting

$$(3.17) \quad \Psi_\gamma(y) = \Psi_\gamma(y; z, r) = S_r^y \bar{\Psi}_\gamma(z, r).$$

If  $e_\gamma$  is an  $(\mathcal{E}'_e(\mathcal{H}^{M,M}), \mathcal{S}_e(\mathcal{H}^{M,M}))$ -mollifier, then

$$S_\gamma Rf := \langle Rf, \Psi_\gamma \rangle_{\mathcal{S}'_r \times \mathcal{S}_r} \rightarrow f$$

for  $f \in \mathcal{E}'_e(\mathcal{H}^{M,M})$ . This means that

$$\langle \langle Rf, \Psi_\gamma \rangle_{\mathcal{S}'_r \times \mathcal{S}_r}, \beta \rangle_{\mathcal{E}'_e(\mathcal{H}^{M,M}) \times \mathcal{S}_e(\mathcal{H}^{M,M})} \rightarrow \langle f, \beta \rangle_{\mathcal{E}'_e(\mathcal{H}^{M,M}) \times \mathcal{S}_e(\mathcal{H}^{M,M})}$$

for all  $\beta \in \mathcal{S}_e(\mathcal{H}^{M,M})$ .

We will construct a general class of  $\bar{e}_\gamma$  in section 4 and show that the resulting  $e_\gamma$  satisfy the definition. We now prove the corollary.

*Proof.* Taking into account (3.17) and (3.14), statement (3.16) is a consequence of

$$e_\gamma(x, y) = S_e^y \bar{e}_\gamma(x) = S_e^y R^* \bar{\Psi}_\gamma(x) = R^* S_r^y \bar{\Psi}_\gamma(x) = R^* \{ \Psi_\gamma(y) \}(x). \quad \square$$

Considering (3.8) a solution of (3.16) is given by  $\bar{\Psi}_\gamma = E\bar{e}_\gamma$ .

REMARK 3.5. *Putting*

$$f_\gamma(y) = \langle f, S_e^y \bar{e}_\gamma \rangle_{\mathcal{S}'_e \times \mathcal{S}_e}$$

it becomes clear from (3.12) that  $\text{supp } f_\gamma \subset \mathcal{H}^M(\mathbb{R}^{n+1})$ . Thus, using the invariance  $S_e^y$  to generate mollifiers, we can only recover objects  $f \in \mathcal{S}'_e$  with support in  $\mathcal{H}^M(\mathbb{R}^{n+1})$ . But this is not a restriction in applications, e.g., in sonar or radar, since the support of any object to be reconstructed is always a positive distance from the line  $y_{n+1} = 0$ . For technical reasons, our mollifiers satisfy the convergence assumption (2.3) for bounded  $|y_{n+1}|$ , so we will reconstruct  $f_\gamma$  only on  $\mathcal{H}^M$  or  $\mathcal{H}^{M,M}$ . This is not a serious practical restriction since  $M$  can be chosen arbitrarily large. Therefore, we will construct  $(\mathcal{E}'_e(\mathcal{H}^{M,M}), \mathcal{S}_e(\mathcal{H}^{M,M}))$ -mollifiers.

To use the method of approximate inverse for inverting  $R$ , we

- choose a mollifier  $e_\gamma$  fulfilling the conditions of Theorem 4.1 defined by  $S_e^y$ :  $e_\gamma(x, y) = S_e^y \bar{e}_\gamma(x)$  and calculate  $\bar{\Psi}_\gamma = E\bar{e}_\gamma$ ;
- compute the approximate inverse of  $R$  as

$$(3.18) \quad S_\gamma g(y) = \langle g, S_r^y \bar{\Psi}_\gamma \rangle_{\mathcal{S}'_r \times \mathcal{S}_r},$$

where  $g = Rf$  are the given data.

Considering (3.9), we have only an explicit representation for  $F E\bar{e}_\gamma$  when  $\rho \geq \|\sigma\|$ . We want to obtain  $\bar{\Psi}_\gamma$  rather than its Fourier transform because a discrete Fourier transform would extend the data, which are given in applications only on a bounded domain, periodically and could cause large artifacts. Furthermore even in the two-dimensional case ( $n = 1$ ) we would have to compute a three-dimensional Fourier transform of the data. Therefore, we need an explicit representation of  $F E\bar{e}_\gamma$  for all  $\rho \geq 0$  and  $\sigma \in \mathbb{R}^n$ . (Andersson uses an extension method from Stein [30] which is fairly arbitrary and not explicit for calculations.) We will present an idea in section 4 that will circumvent these difficulties.

**4. Design of a mollifier for R.** Due to Corollary 3.4 we let the mollifier  $e_\gamma$  be defined  $e_\gamma(x, y) = S_e^y \bar{e}_\gamma(x)$  as in (3.12).

Since we will need the Fourier transform of  $\bar{e}_\gamma$  to compute the reconstruction kernel (see (3.9)) it is appropriate to choose  $\bar{e}_\gamma$  as a tensor product

$$(4.1) \quad \bar{e}_\gamma(x) = e_\gamma^1(x') \otimes e_\gamma^2(x_{n+1}),$$

where  $e_\gamma^1 \in \mathcal{S}(\mathbb{R}^n)$ ,  $e_\gamma^2 \in \mathcal{S}(\mathbb{R})$ ,  $e_\gamma^2$  even. Defining  $e_\gamma(x, y)$  as in (3.15), (4.1) it is obvious that  $e_\gamma(\cdot, y) \in \mathcal{S}_e(\mathbb{R}^{n+1})$  for all  $y \in \mathbb{R}^{n+1}$ .

In view of (3.9) and Theorem 4.1 below we want  $e_\gamma$  and  $\bar{e}_\gamma$  to have the following properties:

1.  $\int_{\mathbb{R}^n} e_\gamma^1(z) dz = 1 = \int_{\mathbb{R}} e_\gamma^2(t) dt$ .
2.  $Fe_\gamma^1$  is easy to calculate.
3.  $Fe_\gamma^2(\sqrt{\xi})$  has a nice extension for  $\xi < 0$ .

By “nice” in 3, we mean that the extension is explicitly known since we do not want to apply an extension lemma [30] like Andersson did it in his article [2]. Moreover we need an explicit expression for that extension to calculate the corresponding reconstruction kernel.

Now we get more explicit with our choices for  $e_\gamma^1$  and  $e_\gamma^2$ . We define

$$(4.2) \quad e_\gamma^1(x') = \gamma^{-n} e^1(x'/\gamma) \quad \text{for } e^1(x') \in \mathcal{S}(\mathbb{R}^n), \quad \int_{\mathbb{R}^n} e^1(z) dz = 1.$$

We have to be careful with respect to the choice of  $e_\gamma^2$ . Let  $F \in \mathcal{S}_e(\mathbb{R})$  have mean value 1. To guarantee the mollifier property, because of the dilation by  $y_{n+1}$  in  $S_e^y$  (see (3.12) and (3.15)), we define

$$(4.3) \quad e_\gamma^2(q) = \frac{1}{2\gamma} \left\{ F\left(\frac{q+1}{\gamma}\right) + F\left(\frac{q-1}{\gamma}\right) \right\} \quad \text{for } F \in \mathcal{S}_e(\mathbb{R}), \quad \int_{\mathbb{R}} F(t) dt = 1.$$

We will show that property 3 is fulfilled when we define  $F$  as in (4.5) below.

The following key theorem asserts that these properties guarantee  $e_\gamma$  is a mollifier. The proof will be given in the appendix.

**THEOREM 4.1.** *Let  $M > 1$  and let functions  $e_\gamma^1$  and  $e_\gamma^2$  be given by (4.2) and (4.3). Then,  $e_\gamma$  defined by (3.15) and (4.1) is an  $(\mathcal{E}'_e(\mathcal{H}^{M,M}), \mathcal{S}_e(\mathcal{H}^{M,M}))$ -mollifier.*

We will now construct specific functions  $e_\gamma^1$  and  $e_\gamma^2$  that we will use in our algorithm. We define

$$(4.4) \quad e_\gamma^1(x') = \gamma^{-n} e^1(x'/\gamma), \quad e^1(x') = (2\pi)^{-n/2} \exp(-\|x'\|^2/2), \quad x' \in \mathbb{R}^n,$$

which obviously is a function in  $\mathcal{S}(\mathbb{R}^n)$  with mean value 1, since  $\int_{\mathbb{R}^n} e_\gamma^1(x') dx' = \hat{e}_\gamma^1(0) = 1$ .

We have to be more careful in the choice of  $e_\gamma^2$ . The desirable extension property 3 for  $e_\gamma^2$  is fulfilled if there exists a function  $g \in \mathcal{S}(\mathbb{R})$  satisfying

$$(4.5) \quad Fe_\gamma^2(\sqrt{\xi}) = g(\xi^2).$$

The function

$$(4.6) \quad F(q) := 2F^{-1}\{\exp(-|\xi|^4)\}(2q)$$

satisfies (4.5) with  $g(\xi) = \exp(-|\xi|^2)$ . So,  $F$  is an even function in  $\mathcal{S}(\mathbb{R})$  with mean value equal to 1. We define  $e_\gamma^2$  using (4.3) and the specific function (4.6).

REMARK 4.2. *Since the inverse Fourier transform of  $\exp(-|\xi|^4)$  does not decrease as rapidly as  $\exp(-|\xi|^2)$  near  $\xi = 0$ , we introduced the dilation factor 2 in (4.6) to make the decay behavior the same in both variables (see also Figure 1).*

COROLLARY 4.3. *Let  $M > 1$ . The function  $e_\gamma = e_\gamma^1 \otimes e_\gamma^2$  defined using (4.4) and (4.3) with  $F$  defined by (4.6) satisfies the assumptions of Theorem 4.1 and therefore is an  $(\mathcal{E}'_e(\mathcal{H}^{M,M}), \mathcal{S}_e(\mathcal{H}^{M,M}))$ -mollifier.*

*Proof.* All we need to do is observe that our specific  $e^1$  and  $F$  satisfy  $\int_{\mathbb{R}^n} e^1(z) dz = 1 = \int_{\mathbb{R}} F(t) dt$  and that  $e_\gamma$  is constructed according to Theorem 4.1.  $\square$

Figure 1 displays  $\bar{e}_\gamma$  in the case of  $n = 1$ ,  $\gamma = 0.06$ . It has its peak in  $(0, 1)$ .

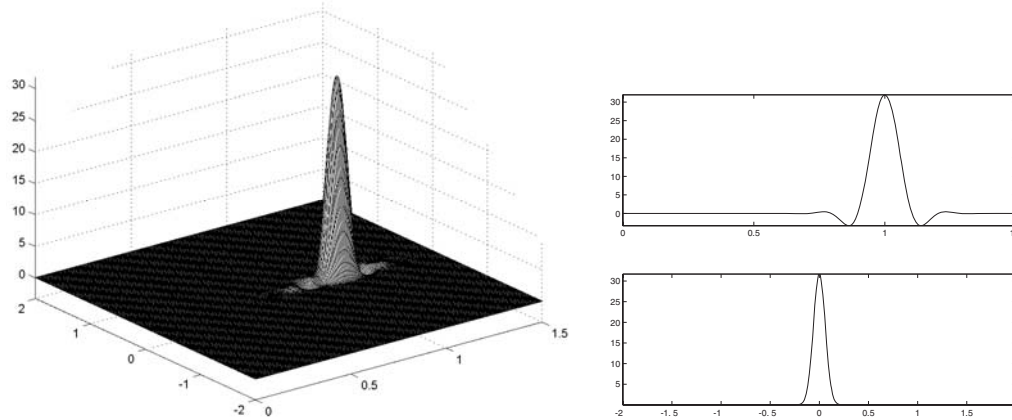


FIG. 1. *Plot of  $e_\gamma(x_1, x_2)$  in the two-dimensional case ( $n = 1$ ) for  $\gamma = 0.06$  (left picture). On the right-hand side is the graph of  $e_\gamma^1$  (bottom) and  $e_\gamma^2$  (top). The width of the peak is about 0.5 units in each case (note the different scales), which is achieved by the dilation in (4.6).*

**5. Computation of the reconstruction kernel  $\bar{\Psi}_\gamma$ .** Throughout this section we assume  $\bar{e}_\gamma$  to be given as in (4.1), (4.2), (4.3), (4.4), and (4.6) and  $e_\gamma(x, y) = \mathcal{S}_e^y \bar{e}_\gamma(x)$ . Our aim is to compute  $\bar{\Psi}_\gamma = E\bar{e}_\gamma$ .

From Lemma 3.2 we know that

$$(5.1) \quad F\bar{\Psi}_\gamma(\sigma, \rho) = FE\bar{e}_\gamma = F\bar{e}_\gamma(\sigma, \sqrt{\rho^2 - \|\sigma\|^2}) \quad \text{if } \rho \geq \|\sigma\|,$$

where  $\rho \geq 0$ ,  $\sigma \in \mathbb{R}^n$ . Thus, we have to compute the Fourier transform of  $\bar{e}_\gamma$  at first.

LEMMA 5.1. *We have that*

$$(5.2) \quad F\bar{e}_\gamma(\sigma, \rho) = \hat{e}_\gamma^1(\sigma) \hat{e}_\gamma^2(\rho) = \cos(\rho) e^{-\gamma^2 \|\sigma\|^2 / 2} e^{-\gamma^4 \rho^4 / 16},$$

where  $\sigma \in \mathbb{R}^n$ ,  $\rho \in \mathbb{R}$ .

*Proof.* The proof follows from a straightforward calculation using the definition of  $\bar{e}_\gamma$ .  $\square$

So far by Lemma 5.1 we have the representation

$$(5.3) \quad F\bar{\Psi}_\gamma(\sigma, \rho) = \cos(\sqrt{\rho^2 - \|\sigma\|^2}) e^{-\gamma^2 \|\sigma\|^2 / 2} e^{-\gamma^4 (\rho^2 - \|\sigma\|^2)^2 / 16} \quad \text{if } \rho \geq \|\sigma\|.$$

To get  $\bar{\Psi}_\gamma$  for all  $\rho \geq 0$  and  $\sigma \in \mathbb{R}^n$ , we have to find an extension of  $\cos \sqrt{\xi}$  for  $\xi < 0$  that turns (5.3) into a function in  $\mathcal{S}_\Gamma$ . The natural extension involves  $\cosh \sqrt{-\xi}$  for  $\xi < 0$ . As noted in section 3, we can extend  $\bar{\Psi}_\gamma$  arbitrarily, and for computational

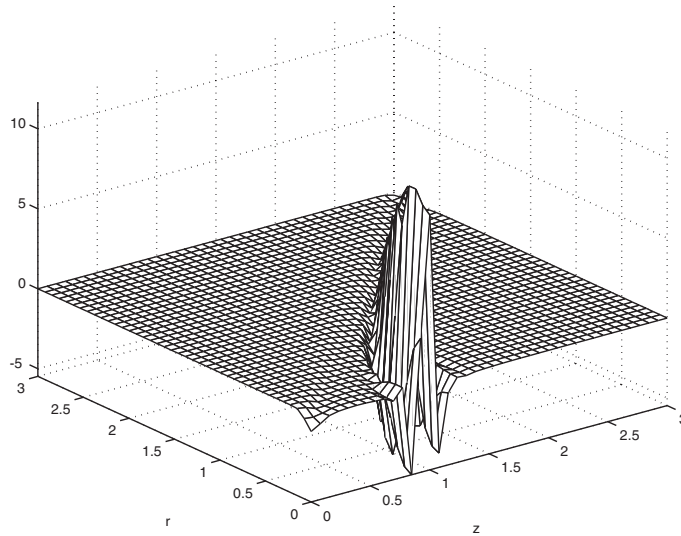


FIG. 2. The reconstruction kernel  $\bar{\Psi}_\gamma$  given as in (5.6) for  $\gamma = 0.06$  and  $n = 1$ . The integrals have been computed using numerical integration.

reasons, we will cut this function off away from  $\xi = 0$ . Let  $\chi \in C^\infty(\mathbb{R})$  be zero on  $(-\infty, -1]$  and 1 on  $[0, \infty)$  and let

$$(5.4) \quad G(\xi) = \begin{cases} \cos \sqrt{\xi}, & \xi \geq 0, \\ \chi(\xi) \cosh(\sqrt{|\xi|}), & \xi < 0. \end{cases}$$

The Fourier transform  $F\bar{\Psi}_\gamma$  is given by

$$(5.5) \quad F\bar{\Psi}_\gamma(\sigma, \rho) = G(\rho^2 - \|\sigma\|^2) e^{-\gamma^2 \|\sigma\|^2 / 2} e^{-\gamma^4 (\rho^2 - \|\sigma\|^2)^2 / 16}$$

and we get  $\bar{\Psi}_\gamma$  by applying the inverse Fourier transform.

LEMMA 5.2. Let  $\bar{e}_\gamma$  be given as in (4.1), (4.2), (4.3), (4.4), and (4.6). Then, a solution of  $R^* \bar{\Psi}_\gamma = \bar{e}_\gamma$  is represented by

$$(5.6) \quad \bar{\Psi}_\gamma(z, r) = 2^n (2\pi)^{-\frac{3}{2}n - \frac{1}{2}} \int_{\mathbb{R}_+^n} \int_0^\infty \left\{ G(\rho^2 - \|\sigma\|^2) e^{-\gamma^2 (\frac{\|\sigma\|^2}{2} + \frac{\gamma^2}{16} (\rho^2 - \|\sigma\|^2)^2)} \cdot \rho^{(n+1)/2} \mathcal{J}_{(n-1)/2}(\rho r) \cos(\langle \sigma, z \rangle) \right\} d\rho d\sigma.$$

Here,  $\mathbb{R}_+^n = \{x = (x_1, \dots, x_n)^\top \in \mathbb{R}^n : x_j \geq 0\}$ ,  $\mathcal{J}_\nu$  is the Bessel function of first kind of order  $\nu$ , and  $G$  is given as in (5.4).

*Proof.* The proof follows by a simple application of an inverse Fourier transform of dimension  $2n + 1$  to (5.5) in which one uses Lemma 5.1, spherical coordinates, and the identity

$$\int_{S^n} e^{i\rho r \langle \omega, \theta \rangle} d\omega = (2\pi)^{(n+1)/2} (\rho r)^{(1-n)/2} \mathcal{J}_{(n-1)/2}(\rho r),$$

which can be found, e.g., in [10].  $\square$

Figure 2 displays a picture of  $\bar{\Psi}_\gamma$  for  $\gamma = 0.06$  and  $n = 1$  corresponding to the two-dimensional case. The integrals in (5.6) have been computed using numerical integration, where the integrals were cut off when the absolute value of the integrand was less than  $10^{-12}$ . The reconstruction kernel in Figure 2 belongs to the mollifier shown in Figure 1 and has its absolute maximum point in  $(0, 1)$ , just as the mollifier  $\bar{e}_\gamma$ .

**6. Implementation and numerical results.** We now have all the ingredients to implement the approximate inverse for the spherical Radon transform. We present results for the two-dimensional case ( $n = 1$ ). The reconstruction kernel  $\bar{\Psi}_\gamma$  (5.6) belonging to the mollifier (4.1), (4.2), (4.3) has the representation

$$(6.1) \quad \bar{\Psi}_\gamma(z, r) = \frac{2}{(2\pi)^2} \left\{ \int_0^\infty \int_0^\infty \tau \mathcal{J}_0(\sqrt{\tau^2 + \sigma^2} r) \cos \tau e^{-\gamma^2 (\frac{\sigma^2}{2} + \frac{\tau^2 \tau^4}{16})} \cos(\sigma z) d\tau d\sigma + \int_0^\infty \int_0^\sigma \tau \mathcal{J}_0(\sqrt{\sigma^2 - \tau^2} r) \chi(-\tau^2) \cosh \tau e^{-\gamma^2 (\frac{\sigma^2}{2} + \frac{\tau^2 \tau^4}{16})} \cos(\sigma z) d\tau d\sigma \right\},$$

where we used the substitutions  $\rho = \sqrt{\tau^2 + \sigma^2}$  and  $\rho = \sqrt{\sigma^2 - \tau^2}$ , respectively.

Throughout this section we suppose that  $f$  has compact support in  $\mathcal{H}^{M,M}(\mathbb{R}^2)$  for a certain  $M > 1$ . The method of approximate inverse used to solve the problem  $\mathbf{R}f = g$  for  $n = 1$  has the form  $S_\gamma \mathbf{R}f(y) = \langle \mathbf{R}f, S_\gamma^y \bar{\Psi}_\gamma \rangle_{S_r^1 \times S_r}$ .

We now adjust the algorithm to practical situations where only finitely many data on a bounded domain are available. Assume that equally spaced centers  $z_k \in [\lambda, \Lambda]$ ,  $\lambda < \Lambda$ ,  $k = 0, \dots, P$ , and equally spaced radii  $r_m \in [0, R]$ ,  $R > 0$ ,  $m = 0, \dots, Q$ , are given, so we have  $N = (P + 1)(Q + 1)$  spherical averages of  $f$  at hand. More explicitly, instead of  $\mathbf{R}f$  itself we have only the vector  $\phi_N \mathbf{R}f \in \mathbb{R}^N$  as data, where  $\phi_N : \mathcal{C}(\mathbb{R} \times [0, \infty)) \rightarrow \mathbb{R}^N$  are the point evaluations

$$(\phi_N v)_{k,m} = v(z_k, r_m), \quad 0 \leq k \leq P, \quad 0 \leq m \leq Q.$$

REMARK 6.1. *The observation operator  $\phi_N$ , which contains all information about the measurement geometry, is well defined only if the function to be evaluated is continuous. Since  $\mathbf{R}f \in S_r^1$  we have to postulate that  $\mathbf{R}f$  is a continuous, but not necessarily integrable, function in order to apply  $\phi_N$  properly. Thus, we assume  $\mathbf{R}f \in \mathcal{C}(\mathbb{R} \times [0, \infty))$  which is not a large restriction since  $\mathbf{R}$  smooths of order  $n/2$  in Sobolev scales.*

To recover  $f$  from  $\phi_N \mathbf{R}f$  we apply the trapezoidal sum corresponding to the nodes  $\{z_k\}, \{r_m\}$  and obtain

$$(6.2) \quad \begin{aligned} S_{\gamma,N} \phi_N \mathbf{R}f(y) &= \langle \phi_N \mathbf{R}f, Q_N \phi_N S_\gamma^y \bar{\Psi}_\gamma \rangle_{\mathbb{R}^N} \\ &= \frac{2\pi}{|y_2|^3} h_z h_r \sum_{k=0}^P \sum_{m=0}^Q r_m \bar{\Psi}_\gamma \left( \frac{z_k - y_1}{|y_2|}, \frac{r_m}{|y_2|} \right) \mathbf{R}f(z_k, r_m) \end{aligned}$$

for  $y \in \mathcal{H}^M(\mathbb{R}^2)$ ,  $Q_N = h_z h_r I_{N,N}$  (compare (2.8)).

Formula (6.2) was applied to get the reconstructions in Figures 3 and 4.

As mentioned in section 5 we compute  $\bar{\Psi}_\gamma$  by applying numerical integration to (6.1) choosing convenient integration boundaries. Moreover we determine  $\bar{\Psi}_\gamma(z, r)$  on the square  $[0, 15]^2$  on an equidistant mesh grid consisting of  $128 \times 128$  grid points. Since the kernel is rapidly decreasing, the absolute value of  $\bar{\Psi}_\gamma$  outside the square

$[0, 15]^2$  is rather small, so we can extend the kernel by 0 there. Using the symmetry  $\bar{\Psi}_\gamma(z, r) = \bar{\Psi}_\gamma(-z, r)$  and linear interpolation we get  $\bar{\Psi}_\gamma(z, r)$  for every  $z \in \mathbb{R}, r \geq 0$ .

To check the performance of the above algorithm we implemented it to reconstruct several objects. All reconstructions were computed for  $(y_1, y_2) \in [0, 7] \times [1, 8]$  using an equidistant mesh grid with  $64 \times 64$  grid points. The objects are assumed to have their support in  $\mathcal{H}^1(\mathbb{R}^2)$ . The data are given on equally spaced points with  $\lambda = -36, \Lambda = 36, P = 384, R = 50,$  and  $Q = 256$ . *Note that in all pictures the  $y_2$ -axis is the horizontal one, whereas the  $y_1$ -axis (the sonar sources, circle centers) is the vertical one.*

First, we recovered the characteristic function of a circle centered at  $(4, 4)$  with radius 1 and density 2. Figure 3 shows the original circle as well as the approximate inverse  $S_{\gamma, N} \phi_N R f$ . We used the reconstruction kernel (6.1) with  $\gamma = 0.06$  which was precomputed for  $(z, r) \in [0, 15]^2$  using  $128 \times 128$  equally distributed grid points.

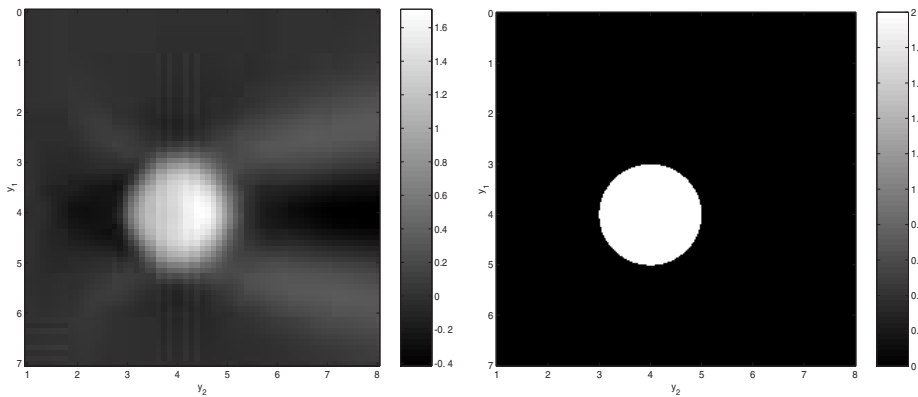


FIG. 3. *Reconstruction of the characteristic function of a circle (left) and original object function (right),  $\gamma = 0.06$ .*

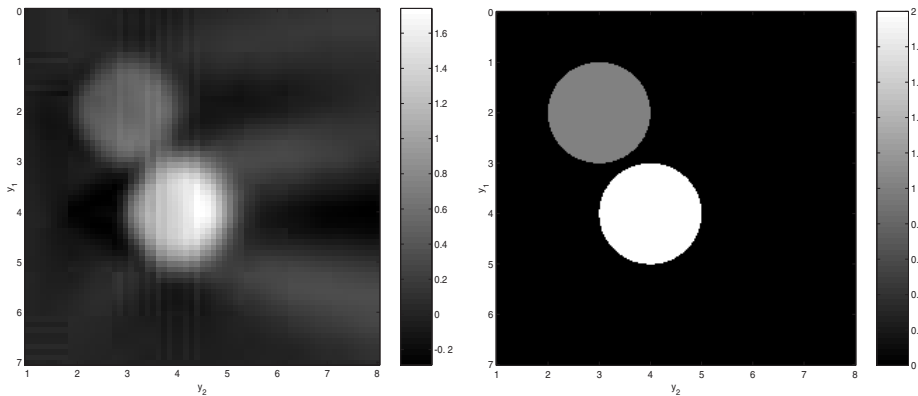


FIG. 4. *Reconstruction of two circles  $f_1$  and  $f_2$  (left) and original object function (right),  $\gamma = 0.06$ .*

Second, we applied the algorithm to the sum of the function in Figure 3 and the characteristic function of a disk centered at  $(2, 3)$  and of radius 1. The reconstruction as well as the original object can be seen in Figure 4; the parameters are the same as

in Figure 3.

These tests show that the method of approximate inverse works fine, and the reconstructions are comparable to those in [9]. Some blurring in the reconstructions is probably caused by the numerical calculation of the reconstruction kernel and truncation error. However, some ill-posedness is inherent in the problem.

REMARK 6.2. *Some of the fuzzy reconstruction boundaries in Figures 3 and 4 are intrinsic to the problem. As shown in [19, 24], the object boundaries that are most difficult to reconstruct are those not tangent to circles in the data set. This means that horizontal boundaries in Figures 3 and 4 will be intrinsically hardest to reconstruct since the set of circle centers is the vertical axis. Since more-or-less vertical boundaries are tangent to spheres in the data set, the microlocal analysis predicts they will be easiest to reconstruct. This is analogous to limited angle X-ray tomography in which some boundaries are “invisible” in the data [25].*

**7. Conclusions.** In this paper we extended the method of approximate inverse, a regularization scheme for operators between Hilbert spaces, to distribution spaces. We applied the method to the inversion problem of the spherical Radon transform which appears in sonar as well as in radar. This algorithm allows one to solve inverse problems for linear operators which are not bounded mappings between Hilbert or Banach spaces.

We presented a representation for a reconstruction kernel  $\bar{\Psi}_\gamma$  in arbitrary dimensions (5.6). Unfortunately, in the three-dimensional case ( $n = 2$ ) numerical integration to get  $\bar{\Psi}_\gamma$  is too time consuming and we are working on other ways to get the reconstruction kernel. In this case a modified inversion formula presented by Klein [13] might be useful. This inversion formula could also be helpful to obtain an *analytic* expression for the reconstruction kernel  $\bar{\Psi}_\gamma$ , which would also increase the accuracy of the reconstructed solution. This and stability and error analysis (as for Hilbert space in [27]) will be part of future research.

**Appendix A. Proof of Theorem 4.1.** Let  $M > 1$ . We recall the general construction of  $e_\gamma$  given in section 4. Let  $e_\gamma(x, y) = \mathcal{S}'_e \bar{e}_\gamma(x)$ , where

$$(A.1) \quad \bar{e}_\gamma(x) = e_\gamma^1(x') \otimes e_\gamma^2(x_{n+1}),$$

$$(A.2) \quad e_\gamma^1(x') = \gamma^{-n} e^1(x'/\gamma), \quad \int_{\mathbb{R}^n} e^1(x') dx' = 1, \quad e^1 \in \mathcal{S}(\mathbb{R}^n),$$

$$(A.3) \quad e_\gamma^2(q) = \frac{1}{2\gamma} \left\{ F\left(\frac{q+1}{\gamma}\right) + F\left(\frac{q-1}{\gamma}\right) \right\} \quad \text{for } F \in \mathcal{S}_e(\mathbb{R}), \quad \int_{\mathbb{R}} F(t) dt = 1.$$

We will use several steps to show that  $e_\gamma$  is an  $(\mathcal{E}'_e(\mathcal{H}^{M,M}), \mathcal{S}_e(\mathcal{H}^{M,M}))$ -mollifier. First, we will prove (2.2) using Lemma A.1. Then, we will prove a distributional Fubini’s theorem, Lemma A.2, and finally, we will prove the convergence result (2.3) which concludes the proof of Theorem 4.1.

LEMMA A.1. *Let  $\gamma > 0$  be fixed,  $e_\gamma$  be defined by (A.1)–(A.3), and  $\varphi \in \mathcal{S}'_e(\mathbb{R}^{n+1})$ . Then, the function  $\langle \varphi, e_\gamma(\cdot, y) \rangle_{\mathcal{S}'_e \times \mathcal{S}_e}$  is a continuous function of polynomial growth for  $y \in \mathcal{H}^M$  and is 0 for  $y \notin \mathcal{H}^M$ . Therefore  $\langle \varphi, e_\gamma(\cdot, y) \rangle_{\mathcal{S}'_e(\mathbb{R}^{n+1}) \times \mathcal{S}_e(\mathbb{R}^{n+1})} \in \mathcal{S}'_e(\mathbb{R}^{n+1})$ .*

*Proof.* First, using the definition of  $e_\gamma$ , one proves the map  $y \mapsto e_\gamma(\cdot, y)$  is a continuous map from  $\mathcal{H}^M$  to  $\mathcal{S}_e(\mathbb{R}^{n+1})$ . Therefore,  $\langle \varphi, e_\gamma(\cdot, y) \rangle_{\mathcal{S}'_e \times \mathcal{S}_e}$  is continuous for  $y \in \mathcal{H}^M$  and is 0 if not.

We simplify the problem by reducing the calculation to integrals of functions. By [6] there exists a multi-index  $\alpha \in \mathbb{N}_0^{n+1}$  and a continuous function  $P_\varphi$  of polynomial

growth such that

$$(A.4) \quad \varphi = D^\alpha P_\varphi,$$

where  $\alpha = (\alpha', \alpha_{n+1})$  and  $D^\alpha = \partial_{x_1}^{\alpha_1} \dots \partial_{x_{n+1}}^{\alpha_{n+1}}$ .

For  $y \in \mathcal{H}^M$ , we obtain

$$(A.5) \quad \begin{aligned} \varphi_\gamma(y) &:= \langle \varphi, e_\gamma(\cdot, y) \rangle_{\mathcal{S}'_e \times \mathcal{S}_e} = (-1)^{|\alpha|} \int_{\mathbb{R}^{n+1}} P_\varphi(x) D_x^\alpha e_\gamma(x, y) dx \\ &= \frac{1}{2(-\gamma|y_{n+1}|)^{|\alpha|}} \int_{\mathbb{R}^n} \int_{\mathbb{R}} \left[ P_\varphi(\gamma|y_{n+1}|z' + y', \gamma|y_{n+1}|z_{n+1} + |y_{n+1}|) \right. \\ &\quad \left. + P_\varphi(\gamma|y_{n+1}|z' + y', \gamma|y_{n+1}|z_{n+1} - |y_{n+1}|) \right] D^{\alpha'} e^1(z') D^{\alpha_{n+1}} F(z_{n+1}) dz_{n+1} dz', \end{aligned}$$

where we used the substitutions  $z' = (x' - y')/(\gamma|y_{n+1}|)$  and  $z_{n+1} = (x_{n+1}/|y_{n+1}| \pm 1)/\gamma$ , as well as the symmetry of  $F$ . Since  $P_\varphi$  is polynomially increasing, there exists a constant  $C_\varphi > 0$  and a  $\kappa > 0$  such that

$$(A.6) \quad |P_\varphi(x)| \leq C_\varphi (1 + \|x\|^2)^\kappa \quad \text{as } \|x\| \rightarrow \infty, \quad x \in \mathbb{R}^{n+1}.$$

Using (A.6) and some simple estimates, we show

$$\left| P_\varphi(\gamma|y_{n+1}|z' + y', \gamma|y_{n+1}|z_{n+1} \pm |y_{n+1}|) \right| \leq C_\varphi 2^\kappa (1 + \gamma^2|y_{n+1}|^2 \|z\|^2)^\kappa (1 + \|y\|^2)^\kappa.$$

This allows us to estimate (A.5) as

$$|\varphi_\gamma(y)| \leq C_\varphi 2^\kappa q_\gamma (\gamma|y_{n+1}|)^{-|\alpha|} (1 + \|y\|^2)^\kappa, \quad y \in \mathcal{H}^M,$$

with  $q_\gamma := \int_{\mathbb{R}^n} \int_{\mathbb{R}} (1 + \gamma^2|y_{n+1}|^2 \|z\|^2)^\kappa D^{\alpha'} e^1(z') D^{\alpha_{n+1}} F(z_{n+1}) dz_{n+1} dz' < \infty$ , which finishes the proof.  $\square$

Our next task is to prove a distributional Fubini's theorem that will allow us to examine the pairing  $\langle e_\gamma(x, \cdot), \beta \rangle$  to show the convergence result (2.3) in Definition 2.1.

LEMMA A.2 (distributional Fubini's theorem). *Let  $\gamma > 0$  be fixed and  $e_\gamma$  be defined by (A.1)–(A.3). Further assume that  $\varphi \in \mathcal{S}'_e(\mathbb{R}^{n+1})$  and  $\beta \in \mathcal{S}_e(\mathcal{H}^M)$ . Then,*

$$(A.7) \quad \begin{aligned} \langle \langle \varphi, e_\gamma(\cdot, y) \rangle_{\mathcal{S}'_e(\mathbb{R}^{n+1}) \times \mathcal{S}_e(\mathbb{R}^{n+1})}, \beta \rangle_{\mathcal{S}'_e(\mathbb{R}^{n+1}) \times \mathcal{S}_e(\mathcal{H}^M)} \\ = \langle \varphi, \langle e_\gamma(x, \cdot), \beta \rangle_{\mathcal{S}'_e(\mathbb{R}^{n+1}) \times \mathcal{S}_e(\mathcal{H}^M)} \rangle_{\mathcal{S}'_e(\mathbb{R}^{n+1}) \times \mathcal{S}_e(\mathbb{R}^{n+1})}. \end{aligned}$$

Furthermore,

$$(A.8) \quad \beta_\gamma(x) := \langle e_\gamma(x, \cdot), \beta \rangle_{\mathcal{S}'_e(\mathbb{R}^{n+1}) \times \mathcal{S}_e(\mathcal{H}^M)} \in \mathcal{S}_e(\mathbb{R}^{n+1}).$$

Note that here,  $\beta_\gamma$  is a function of  $x$ , and in section 2,  $f_\gamma$  is a function of  $y$ .

*Proof.* We reduce this to a Fubini theorem for functions. Since  $\varphi = D^\alpha P_\varphi$  for a function  $P_\varphi$  with polynomial growth by (A.4), we can again use (A.5) to write

$$(A.9) \quad \langle \varphi_\gamma, \beta \rangle_{\mathcal{S}'_e(\mathbb{R}^{n+1}) \times \mathcal{S}_e(\mathcal{H}^M)} = \int_{\mathcal{H}^M} \int_{\mathbb{R}^n} \int_{\mathbb{R}} I_\varphi^\gamma(y', y_{n+1}, x', x_{n+1}) dx_{n+1} dx' dy_{n+1} dy',$$

where

$$I_\varphi^\gamma(y', y_{n+1}, x', x_{n+1}) := \frac{(-1)^{|\alpha|}}{2} (\gamma |y_{n+1}|)^{-n-1-|\alpha|} \beta(y', y_{n+1}) P_\varphi(x', x_{n+1}) \cdot (D^{\alpha'} e^1) \left( \frac{x' - y'}{\gamma |y_{n+1}|} \right) \left\{ (D^{\alpha_{n+1}} F) \left( \frac{x_{n+1} - |y_{n+1}|}{\gamma |y_{n+1}|} \right) + (D^{\alpha_{n+1}} F) \left( \frac{x_{n+1} + |y_{n+1}|}{\gamma |y_{n+1}|} \right) \right\}.$$

Using (A.6),  $y \in \mathcal{H}^M$ , the fact that  $F$ ,  $\beta$ , and  $e^1$  are in  $\mathcal{S}_e$ , and some basic inequalities (e.g.,  $(1 + \|a - b\|^2)^{-q} \leq 2^q (1 + \|b\|^2)^q (1 + \|a\|^2)^{-q}$ ,  $a, b \in \mathbb{R}^n$ ,  $q \in \mathbb{N}$ ), we may estimate

$$\begin{aligned} |I_\varphi^\gamma(y', y_{n+1}, x', x_{n+1})| &\leq (C_\varphi/2) (1 + \|x\|^2)^\kappa (\gamma/M)^{-n-1-|\alpha|} |\beta(y', y_{n+1})| \\ &\cdot \left( 1 + \frac{\|x' - y'\|^2}{\gamma^2 y_{n+1}^2} \right)^{-q_1} \left\{ \left( 1 + \frac{(x_{n+1} - |y_{n+1}|)^2}{\gamma^2 y_{n+1}^2} \right)^{-q_2} + \left( 1 + \frac{(x_{n+1} + |y_{n+1}|)^2}{\gamma^2 y_{n+1}^2} \right)^{-q_2} \right\} \\ &\leq \frac{C_\varphi}{2} \frac{(1 + \|x\|^2)^\kappa}{(1 + \|y\|^2)^{q_3}} \left( \frac{\gamma}{M} \right)^{-n-1-|\alpha|} \frac{(1 + \|y'\|^2)^{q_1}}{(1 + \|x'\|^2)^{q_1}} \frac{(1 + |y_{n+1}|^2)^{q_2}}{(1 + |x_{n+1}|^2)^{q_2}} [2(1 + \gamma^2 y_{n+1}^2)]^{q_1+q_2} \end{aligned}$$

for arbitrary  $q_1, q_2, q_3 \in \mathbb{N}$ .

We see for sufficiently large  $q_1, q_2, q_3$  that the integrand in (A.9) is bounded by an integrable function in  $(x, y) \in \mathbb{R}^{n+1} \times \mathcal{H}^M$ .

This allows us to switch the order of integration in (A.9). Since the integral in this switched version is smooth with uniformly integrable derivatives in  $y \in \mathcal{H}^M$  for  $x$  in any compact set, we can pull the  $D^\alpha$  out of the inner integral. Finally, we use the definition of derivative on  $\mathcal{S}'_e$  to prove (A.7).

To show (A.8), we let  $\alpha \in \mathbb{N}_0^{n+1}$  be an arbitrary multi-index. We will prove that  $D^\alpha \beta_\gamma$  decreases rapidly. We bring the  $D^\alpha$  inside the integral for  $\beta_\gamma$  and use estimates as above, and we find a constant  $\tilde{c}_\gamma > 0$  such that

$$|D^\alpha \beta_\gamma(y)| \leq \tilde{c}_\gamma (1 + \|y'\|^2)^{-q_1} (1 + y_{n+1}^2)^{-q_2}, \quad (y', y_{n+1}) \in \mathbb{R}^{n+1},$$

for arbitrary numbers  $q_1, q_2 \in \mathbb{N}$  since  $\beta \in \mathcal{S}_e(\mathcal{H}^M)$  and  $\gamma$  is fixed. Now, using similar arguments as for the bound on  $|I_\varphi^\gamma|$ , we prove assertion (A.8).  $\square$

The final key is the following important convergence result.

**LEMMA A.3.** *Let  $e_\gamma$  be defined by (A.1)–(A.3). Let  $\beta \in \mathcal{S}_e(\mathcal{H}^{M,M})$  and  $\alpha \in \mathbb{N}_0^{n+1}$  be a multi-index. Assume that  $\beta_\gamma$  is defined by (A.8). Then,  $D^\alpha \beta_\gamma \rightarrow D^\alpha \beta(x)$  pointwise in  $\mathcal{H}^{M,M}$ , and  $D^\alpha \beta_\gamma$  is uniformly bounded in  $(x, \gamma) \in \mathcal{H}^{M,M} \times (0, 1)$ .*

*Proof.* We first use the symmetry of  $F$  to write

$$(A.10) \quad \beta_\gamma(x) = \int_{\mathcal{H}^{M,M}} \frac{1}{(\gamma |y_{n+1}|)^{n+1}} e^1 \left( \frac{x' - y'}{\gamma |y_{n+1}|} \right) F \left( \frac{\begin{pmatrix} x_{n+1} \\ y_{n+1} \end{pmatrix} - 1}{\gamma} \right) \beta(y) dy_{n+1} dy'.$$

We assume  $(x, y) \in \mathcal{H}^{M,M} \times \mathcal{H}^{M,M}$  and then we use the change of variables

$$(A.11) \quad z' = (x' - y') / (|y_{n+1}| \gamma), \quad z_{n+1} = \left( \frac{x_{n+1}}{y_{n+1}} - 1 \right) / \gamma,$$

and we have the following simple but important estimate:

$$(A.12) \quad \frac{1}{M^2} < \frac{1}{M|x_{n+1}|} < \frac{1}{|\gamma z_{n+1} + 1|} < \frac{M}{|x_{n+1}|} < M^2.$$

Then, the integral in (A.10) becomes

$$(A.13) \quad \beta_\gamma(x) = \int_{\mathbb{R}^n} \int_{1/|\gamma z_{n+1}+1| < M^2} e^1(z') F(z_{n+1}) \cdot \beta\left(x' - \frac{\gamma|x_{n+1}|}{|\gamma z_{n+1}+1|} z', \frac{x_{n+1}}{\gamma z_{n+1}+1}\right) \frac{1}{|\gamma z_{n+1}+1|} dz' dz_{n+1},$$

where the limits of integration in (A.13) are determined because  $1/M < |y_{n+1}| < M$  and  $\text{supp } \beta \subset \mathbb{R}^n \times [1/M, M]$ .

In order to subtract  $\beta(x)$  within the integral (A.13), we define an auxiliary function that simplifies the calculation,

$$b_\gamma(x) = \beta(x) \int_{1/|\gamma z_{n+1}+1| < M^2} e^1(z') F(z_{n+1}) \frac{1}{|\gamma z_{n+1}+1|} dz_{n+1}.$$

We must calculate  $D^\alpha[\beta_\gamma - b_\gamma]$  and show this difference goes to zero as  $\gamma \rightarrow 0$ . To do this, we take the derivative inside the integral:

$$(A.14) \quad D^\alpha[\beta_\gamma(x) - b_\gamma(x)] = \int_{\mathbb{R}^n} \int_{1/|\gamma z_{n+1}+1| < M^2} e^1(z') F(z_{n+1}) \cdot D_x^\alpha \left\{ \beta\left(x' - \frac{\gamma|x_{n+1}|}{|\gamma z_{n+1}+1|} z', \frac{x_{n+1}}{\gamma z_{n+1}+1}\right) - \beta(x) \right\} \frac{1}{|\gamma z_{n+1}+1|} dz' dz_{n+1}.$$

To show that (A.14) converges to zero, we must do two things:

1. We need to show for each  $x \in \mathcal{H}^{M,M}$  that the integrand in (A.14) is bounded by an integrable function uniformly in  $\gamma \in (0, 1)$ .
2. We need to show  $D^\alpha \beta_\gamma$  is bounded by an integrable function, uniformly in  $\gamma \in (0, 1)$ .

To show 1, we need to examine the derived integrand. The  $D_{x'}^{\alpha'}$  terms are evaluated on  $\beta$  in both terms of (A.14) and they do not cause a problem, so we will evaluate them first. This gives an expression

$$(A.15) \quad D_x^\alpha \left\{ \beta\left(x' - \frac{\gamma|x_{n+1}|}{|\gamma z_{n+1}+1|} z', \frac{x_{n+1}}{\gamma z_{n+1}+1}\right) - \beta(x) \right\} = D_{x_{n+1}}^{\alpha_{n+1}} (D_{x'}^{\alpha'} \beta) \left(x' - \frac{\gamma|x_{n+1}|}{|\gamma z_{n+1}+1|} z', \frac{x_{n+1}}{\gamma z_{n+1}+1}\right) - D_x^\alpha \beta(x).$$

However, because  $x_{n+1}$  appears in both coordinates of the first  $\beta$  in (A.15), some of the derivatives in  $D_{x_{n+1}}^{\alpha_{n+1}}$  fall on the first coordinate. We will let  $\delta' = (\delta_1, \dots, \delta_n)$  denote a multi-index in  $\mathbb{N}_0^n$ . An explicit calculation shows that the integrand in (A.14) can be written for  $x_{n+1} > 1/M > 0$  as a sum of terms in which some derivatives in  $x_{n+1}$  fall on the first coordinates of  $\beta$  and then the term in which all derivatives fall on the last coordinate, the integrand in (A.14) becomes

$$(A.16) \quad \frac{e^1(z') F(z_{n+1})}{|\gamma z_{n+1}+1|} \left[ \sum_{0 < |\delta'| \leq \alpha_{n+1}} \left( \frac{\gamma^{|\delta'|} (-z)^{\delta'}}{|\gamma z_{n+1}+1|^{|\delta'|} (\gamma z_{n+1}+1)^{\alpha_{n+1}-|\delta'|}} \cdot \left( \partial_{x_{n+1}}^{\alpha_{n+1}-|\delta'|} D_{x'}^{\delta'+\alpha'} \beta \right) \left(x' - \frac{\gamma|x_{n+1}|}{|\gamma z_{n+1}+1|} z', \frac{x_{n+1}}{\gamma z_{n+1}+1}\right) \right) + \left\{ (\gamma z_{n+1}+1)^{-\alpha_{n+1}} (D^\alpha \beta) \left(x' - \frac{\gamma|x_{n+1}|}{|\gamma z_{n+1}+1|} z', \frac{x_{n+1}}{\gamma z_{n+1}+1}\right) - D^\alpha \beta(x) \right\} \right].$$

A similar formula is obtained for  $x_{n+1} < -1/M < 0$ .

Because  $1/|\gamma z_{n+1} + 1| \leq M^2$ , it can be seen from (A.16) that the integrand of (A.14) can be bounded by an integrable function uniformly in  $\gamma \in (0, 1)$ . Hence, an application of Lebesgue's dominated convergence theorem shows  $D^\alpha(\beta_\gamma - b_\gamma) \rightarrow 0$  pointwise for  $x \in \mathcal{H}^{M,M}$ . This is valid for two reasons: the sum in (A.16) is a factor of  $\gamma$  times a bounded function, and the difference in braces goes to zero as  $\gamma \rightarrow 0$ . Since  $(b_\gamma - \beta) \rightarrow 0$  in  $\mathcal{S}_e(\mathcal{H}^{M,M})$  we thus have  $D^\alpha(\beta_\gamma - \beta) \rightarrow 0$  pointwise in  $\mathcal{H}^{M,M}$ .

A similar boundedness argument shows that  $D^\alpha\beta_\gamma$  is bounded by an integrable function uniformly in  $\gamma \in (0, 1)$ .  $\square$

At last, we finish the proof of Theorem 4.1. Recall that in the statement of this theorem,  $\varphi$  has compact support in  $\mathcal{H}^{M,M}$  and  $\varphi = D^\alpha P_\varphi$  for a function  $P_\varphi$  of polynomial growth (A.4). Thus, there are compactly supported functions  $\psi_1(x')$  and  $\psi_2(x_{n+1})$  such that  $\psi_2$  is one on  $[-M, -1/M] \cup [1/M, M]$  and supported in  $[-2M, -1/2M] \cup [1/2M, 2M]$  and  $\psi(x) = \psi_1(x')\psi_2(x_{n+1})$  is one on a neighborhood of  $\text{supp } \varphi$ . Then,  $\varphi = \psi D^\alpha P_\varphi$ .

By Lemma A.2,

$$\begin{aligned} \langle \varphi_\gamma, \beta \rangle_{\mathcal{S}'_e(\mathbb{R}^{n+1}) \times \mathcal{S}_e(\mathcal{H}^{M,M})} &= \langle \varphi, \beta_\gamma \rangle_{\mathcal{S}'_e(\mathcal{H}^{M,M}) \times \mathcal{S}_e(\mathbb{R}^{n+1})} \\ (A.17) \qquad \qquad \qquad &= (-1)^{|\alpha|} \int_{\mathcal{H}^{M,M}} P_\varphi(x) D^\alpha \{ \psi(x) \beta_\gamma(x) \} dx. \end{aligned}$$

By the product rule for derivatives and the convergence result Lemma A.3, we see that the derivative in (A.17) converges pointwise on any compact set in  $x$ , and it is uniformly bounded. Therefore, we can use Lebesgue's dominated convergence theorem again to finish the proof of Theorem 4.1.

**Acknowledgments.** The authors are indebted to Jens Klein, Aleksei Beltukov, and Alfred Louis for very useful conversations. The authors are grateful to the referees and editors, in particular Adel Faridani, for thoughtful comments that improved the article.

#### REFERENCES

- [1] M. AGRANOVSKY AND E. T. QUINTO, *Injectivity sets for Radon transform over circles and complete systems of radial functions*, J. Funct. Anal., 139 (1996), pp. 383–414.
- [2] L.-E. ANDERSSON, *On the determination of a function from spherical averages*, SIAM J. Math. Anal., 19 (1988), pp. 214–232.
- [3] R. BARAKAT, *Private communication*, 1997.
- [4] A. BELTUKOV, *Sonar Transforms*, Ph. D. thesis, Tufts University, Medford, MA, 2004.
- [5] M. CHENEY, *Tomography problems arising in Synthetic Aperture Radar*, in Radon Transforms and Tomography, Contemp. Math. 278, AMS, Providence, RI, 2001, pp. 15–28.
- [6] F. CONSTANTINESCU, *Distributions and Their Applications in Physics*, Teubner, Leipzig, 1974.
- [7] R. COURANT AND D. HILBERT, *Methods of Mathematical Physics*, Vol. II, Wiley-Interscience, New York, 1962.
- [8] A. DENISJUK, *Integral geometry on the family of semi-spheres*, Fract. Calc. Appl. Anal., 2 (1999), pp. 31–46.
- [9] A. DENISJUK, *On Numerical Reconstruction of a Function by Its Arc Means with Incomplete Data*, Tech. report, Brest State University, Belarus, 1999.
- [10] J. FAWCETT, *Inversion of n-dimensional spherical averages*, SIAM J. Appl. Math., 45 (1985), pp. 336–341.
- [11] D. FINCH, S. K. PATCH, AND RAKESH, *Determining a function from its mean values over a family of spheres*, SIAM J. Math. Anal., 35 (2004), pp. 1213–1240.
- [12] F. JENSEN, W. KUPERMAN, M. PORTER, AND H. SCHMIDT, *Computational Ocean Acoustics*, AIP Press, Springer, New York, 2000.

- [13] J. KLEIN, *Inverting the spherical Radon transform for physically meaningful functions*, preprint, Westfälische Wilhelms-Universität, Institut für Numerische und Instrumentelle Mathematik, Münster, Germany, 2003. Available online from <http://www.arachne.uni-muenster.de:8000/num/Preprints/2003/kleinje/>.
- [14] R. KRUEGER, D. REINECKE, AND G. KRUEGER, *Thermoacoustic computed tomography*, *Med. Phys.*, 26 (1999), pp. 1832–1837.
- [15] M. LAVRENTIEV, V. ROMANOV, AND V. VASILIEV, *Multidimensional Inverse Problems for Differential Equations*, *Lecture Notes in Math.* 167, Springer-Verlag, New York, 1970.
- [16] A. LOUIS, *Approximate inverse for linear and some nonlinear problems*, *Inverse Problems*, 12 (1996), pp. 175–190.
- [17] A. LOUIS, *A unified approach to regularization methods for linear ill-posed problems*, *Inverse Problems*, 15 (1999), pp. 489–498.
- [18] A. LOUIS AND P. MAASS, *A mollifier method for linear operator equations of the first kind*, *Inverse Problems*, 6 (1990), pp. 427–440.
- [19] A. LOUIS AND E. T. QUINTO, *Local tomographic methods in SONAR*, in *Surveys on Solution Methods for Inverse Problems*, D. Colton, H. Engl, A. Louis, J. McLaughlin, and W. Rundell, eds., Springer, Vienna, 2000, pp. 147–154.
- [20] M. NESSIBI, L. RACHDI, AND K. TRIMECHE, *Ranges and inversion formulas for spherical mean operator and its dual*, *J. Math. Anal. Appl.*, 196 (1995), pp. 861–884.
- [21] S. NORTON, *Reconstruction of a reflectivity field from line integrals over circular paths*, *J. Acoust. Soc. Amer.*, 67 (1980), pp. 853–863.
- [22] S. NORTON, *Reconstruction of a two-dimensional reflecting medium over a circular domain: Exact solution*, *J. Acoust. Soc. Amer.*, 67 (1980), pp. 1266–1273.
- [23] S. NORTON AND M. LINZER, *Ultrasonic reflectivity imaging in three dimensions: Exact inverse scattering solutions for plane, cylindrical, and spherical apertures*, *IEEE Trans. Biomed. Engrg.*, 28 (1981), pp. 200–202.
- [24] V. PALAMODOV, *Reconstruction from limited data of arc means*, *J. Fourier Anal. Appl.*, 6 (2000), pp. 26–42.
- [25] E. T. QUINTO, *Singularities of the X-ray transform and limited data tomography in  $\mathbb{R}^2$  and  $\mathbb{R}^3$* , *SIAM J. Math. Anal.*, 24 (1993), pp. 1215–1225.
- [26] A. RAMM, *Injectivity of the spherical mean operator*, *C. R. Math. Acad. Sci. Paris*, 335 (2002), pp. 1033–1038.
- [27] A. RIEDER AND T. SCHUSTER, *The approximate inverse in action II*, *Math. Comp.*, 72 (2003), pp. 1399–1415.
- [28] A. RIEDER AND T. SCHUSTER, *The approximate inverse in action III: 3D-Doppler tomography*, *Numer. Math.*, 97 (2004), pp. 353–378.
- [29] W. RUDIN, *Functional Analysis*, McGraw-Hill, New York, 1973.
- [30] E. STEIN, *Singular Integrals and Differentiability Properties of Functions*, Princeton University Press, Princeton, NJ, 1970.